
Variational Positive-incentive Noise: How Noise Benefits Models

Hongyuan Zhang Sida Huang Xuelong Li*

School of Artificial Intelligence, OPTics and ElectroNics (iOPEN)

Northwestern Polytechnical University

hyzhang98@gmail.com sidahuang2001@163.com li@nwpu.edu.cn

Abstract

A large number of works aim to alleviate the impact of noise due to an underlying conventional assumption of the negative role of noise. However, some existing works show that the assumption does not always hold. In this paper, we investigate how to benefit the classical models by random noise under the framework of Positive-incentive Noise (*Pi-Noise*) [1]. Since the ideal objective of Pi-Noise is intractable, we propose to optimize its variational bound instead, namely variational Pi-Noise (*VPN*). With the variational inference, a VPN generator implemented by neural networks is designed for enhancing base models and simplifying the inference of base models, without changing the architecture of base models. Benefiting from the independent design of base models and VPN generators, the VPN generator can work with most existing models. From the experiments, it is shown that the proposed VPN generator can improve the base models. It is appealing that the trained variational VPN generator prefers to blur the irrelevant ingredients in complicated images, which meets our expectations.

1 Introduction

Although there are plenty of works aiming to promote the deep models via eliminating the noise contained in data, some studies [2, 3, 4, 5, 6, 7, 8] have explicitly or implicitly shown the potential positive effect of noise [4]. Motivated by Positive-incentive Noise (*Pi-Noise*) [1], we focus on the framework that formally analyzes noise using information theory. For simplicity, we use π -noise to denote pi-noise in the rest of this paper. The noise that simplifies the task is defined as π -noise. Formally speaking, the noise $\varepsilon \in \mathcal{E}$ satisfying

$$I(\mathcal{T}, \mathcal{E}) > 0 \Leftrightarrow H(\mathcal{T}) > H(\mathcal{T}|\mathcal{E}) \quad (1)$$

is defined as π -noise to the task \mathcal{T} , where $H(\cdot)$ represents the information entropy and $I(\cdot, \cdot)$ denotes the mutual information. Noise is named as pure noise provided that $I(\mathcal{T}, \mathcal{E}) = 0$. Although adding some random noise is sometimes regarded as an optional data augmentation method, it is an unstable scheme in practice. Following this principle, it becomes possible to definitely predict whether a class of distributions would benefit the target task \mathcal{T} . It is counterintuitive and attractive that some random noise would benefit the task, rather than disturbing it.

The crux of π -noise is how to properly define the task entropy $H(\mathcal{T})$ and efficiently calculate it. As a basic task of machine learning, the task entropy of single-label classification is relatively easy and direct to model. It may be a rational scheme to measure the complexity of a classification task by computing the uncertainty of labels. In other word, the entropy of $p(y|\mathbf{x})$ is a crucial quantity related to the task complexity and it is formulated as

$$H(p(y|\mathbf{x})) = \int -p(y|\mathbf{x}) \log p(y|\mathbf{x}) dy. \quad (2)$$

*Corresponding author

Remark that y is assumed as a continuous variable for mathematical convenience, which implies the infinite classes, and the integral operation can be simply substituted by the summation if there are finite number of classes. In most scenarios, the labels annotated by humans are regarded as the true $p(y|\mathbf{x})$, *i.e.*, a one-hot distribution. On more complicated datasets such as ImageNet [9], the one-hot property may be not the optimal setting for $p(y|\mathbf{x})$. For example, an image with complicated background may be assigned to diverse labels with different probabilities. It should be pointed out that $p(y|\mathbf{x})$ is different from multi-label classification [10], which allows assigning multiple labels to a data point. This paper focuses on the single-label classification and the purpose of defining $p(y|\mathbf{x})$ is to better predict a label for each sample.

The primary challenges of the π -noise principle are concluded as the following two aspects:

- C1*: Since there are integrals of several continuous variables (*e.g.*, ε) in mutual information, the computation is usually intractable.
- C2*: Precise $p(y|\mathbf{x})$ is unavailable since every data point has only one label as its ground truth on single-label classification datasets.

In this paper, we apply the variational inference technique to π -noise, namely Variational Pi-Noise (*VPN*). Via optimizing the variational bound, challenge *C1* is addressed. Using the Monte Carlo method, we can train a π -noise generator without precise $p(y|\mathbf{x})$, which partially addresses challenge *C2*. The *VPN* generator learns the probability density function of noise and is implemented by neural networks. It can be applied to any existing models designed for task \mathcal{T} (namely base models). A trained *VPN* generator can produce any amount of noise for any sample. It can be, thereby, used in both the training and inference phases of base models. The effectiveness of *VPN* is verified by experiments. From the experimental visualization, we surprisingly find that the generated π -noise prefers to blur the irrelevant background of complicated images, which meets our expectation of the task entropy and mutual information.

Notations In this paper, \mathcal{X} , \mathcal{Y} , and \mathcal{E} represent the sample space, label space, and noise space, respectively. The vector is denoted by lower-case letter in bold and matrix is denoted by upper-case letter in bold. \mathbf{I} is the identity matrix. $\mathcal{N}(\boldsymbol{\mu}, \boldsymbol{\Sigma})$ is the multivariate Gaussian distribution with the mean vector $\boldsymbol{\mu}$ and correlation matrix $\boldsymbol{\Sigma}$. $x \rightarrow y \rightarrow z$ is a Markov chain. \mathbb{R}_+ is the set of non-negative real numbers. \circ represents the composition operation of two functions and \odot is the Hadamard product. We simply use \int to represent both single and multiple Riemann integral, while $\int_E^{(L)} \cdot dx$ represents a Lebesgue integral on E .

2 Related Work

One may be confused about the difference between π -noise and conventional data augmentation [11] (such as translation, rotation, noising, and shearing of vision data), which are particularly prevalent on account of contrastive learning [12, 13]. The data augmentation only participates in the training phase and the testing sample is inputted without augmentation during the inference phase. In *VPN*, we train a generator that can produce π -noise for both the training and inference phases. In other words, one may use a well-trained *VPN* generator to automatically generate π -noise for any unseen samples and help the base model to distinguish the sophisticated samples, which is appealing compared with the conventional data augmentation.

There is another kind of popular learnable augmentation method [14, 15], which is widely applied in recent years: adversarial training. Adversarial training [4] is a hot topic to promote the robustness of deep models. It aims at adding perturbations (namely adversarial attack), during training deep models, to the input of neural network to lead the network to output the incorrect prediction with high confidence. For example, FSGM [16], a white-box method, generates the attack regarding the gradient of x . One pixel attack [17], a black-box method, only changes a pixel of an input image. The procedure of adversarial training is somewhat similar to π -noise. The primary difference is the purpose and impact of noise. The perturbations for adversarial attack are used to fool base models while π -noise is employed to enhance base models. From the optimization aspect, adversarial perturbations try to maximize the loss while π -noise can be regarded as minimizing it instead. Under the π -noise framework [1], adversarial perturbations should be classified as pure noise.

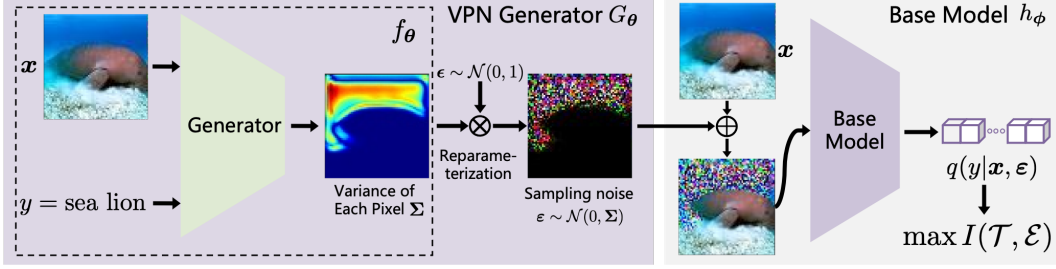


Figure 1: The illustration of VPN framework, which consists of a base model and a π -noise generator. The generator can be trained either with the base model or after the base model. Any model that can predict $p(y|\mathbf{x})$ could be a valid base model.

The variational inference used in this paper is a practical technique in machine learning, especially in variational auto-encoder (VAE) [18], variational information bottleneck (VIB) [19], and their extensions [20]. In particular, VIB attempts to maximize the mutual information between the label y and latent representation z and meanwhile minimize the mutual information between y and input representation x . However, VIB is essentially different from the proposed VPN. On the one hand, $y \rightarrow x \rightarrow z$ is a core assumption of VIB, while there is no assumption of conditional independence in the proposed VPN, which will be elaborated in the succeeding section. On the other hand, VIB essentially provides a new training principle for deep models to learn more informative and concise representations. In comparison, VPN introduces a new module, namely VPN generator. The architecture of VPN generator could be independent of the base deep models. The base models can either be co-trained with VPN generator or stay unchanged during training generator.

3 Variational Positive-incentive Noise

The goal of this paper is to develop a practical paradigm to generate π -noise so that the base models for task \mathcal{T} can be fed with data and the related π -noise. Remark that the added module learning π -noise would not change the architecture of base models. In summary, we expect to learn a probability density function (pdf) parameterized by θ , $\mathcal{D}_\theta : \mathcal{X} \times \mathcal{Y} \mapsto \mathbb{R}_+$, which are trained with the base model, to produce π -noise that benefits the base model. Accordingly, the original training objective of learning π -noise is

$$\max_{\theta} I(\mathcal{T}, \mathcal{E}), \quad s.t. \forall \mathbf{x} \in \mathcal{X}, y \in \mathcal{Y}, \varepsilon \sim \mathcal{D}_\theta(\mathbf{x}, y). \quad (3)$$

The *whole module* consisting of learning \mathcal{D}_θ and sampling from \mathcal{D}_θ is named as the π -noise generator, denoted by G_θ . The base model is denoted by h_ϕ where ϕ is its learnable parameters. The whole procedure is illustrated in Figure 1.

3.1 Define Task Entropy over Distribution $\mathcal{D}_\mathcal{X}$

To begin with, we first define task entropy over the data distribution, which is represented as $\mathcal{D}_\mathcal{X}$,

$$H(\mathcal{T}) = \mathbb{E}_{\mathbf{x} \sim \mathcal{D}_\mathcal{X}} H(p(y|\mathbf{x})) = \int -p(\mathbf{x})p(y|\mathbf{x}) \log p(y|\mathbf{x}) d\mathbf{x}dy. \quad (4)$$

With the formal definition of $H(\mathcal{T})$, the mutual information over $\mathcal{D}_\mathcal{X}$ can be defined as

$$I(\mathcal{T}, \mathcal{E}) = \mathbb{E}_{\mathbf{x} \sim \mathcal{D}_\mathcal{X}} \int p(y, \varepsilon|\mathbf{x}) \log \frac{p(y, \varepsilon|\mathbf{x})}{p(y|\mathbf{x}) \cdot p(\varepsilon|\mathbf{x})} dyd\varepsilon \quad (5)$$

$$= \int p(\mathbf{x})p(y, \varepsilon|\mathbf{x}) \log \frac{p(y, \varepsilon|\mathbf{x})}{p(y|\mathbf{x}) \cdot p(\varepsilon|\mathbf{x})} dyd\varepsilon d\mathbf{x} \quad (6)$$

$$= \int p(\mathbf{x})p(y, \varepsilon|\mathbf{x}) \log \frac{p(y|\mathbf{x}, \varepsilon)}{p(y|\mathbf{x})} dyd\varepsilon d\mathbf{x}. \quad (7)$$

It should be clarified that we do not define the task entropy on the given dataset $\{\mathbf{x}_i\}_{i=1}^n$ as $\sum_{i=1}^n H(p(y|\mathbf{x}_i)) = -\sum_{i=1}^n \int p(y|\mathbf{x}_i) \log p(y|\mathbf{x}_i) dy$, which is easily extended from Eq. (2). The

advantages to define $H(\mathcal{T})$ on $\mathcal{D}_{\mathcal{X}}$ are mainly from two aspects. On the one hand, the definition on a data distribution is a more reasonable setting. On the other hand, the expectation can lead to a brief mathematical formulation after applying the Monte Carlo method, which will be shown in Eq. (15). By reformulating $I(\mathcal{T}, \mathcal{E})$ as follows

$$I(\mathcal{T}, \mathcal{E}) = \int p(\mathbf{x})p(y, \boldsymbol{\varepsilon}|\mathbf{x}) \log p(y|\mathbf{x}, \boldsymbol{\varepsilon})dyd\boldsymbol{\varepsilon}d\mathbf{x} - \int p(y, \mathbf{x}) \log p(y|\mathbf{x})dyd\mathbf{x} \quad (8)$$

$$= \int p(\mathbf{x})p(y, \boldsymbol{\varepsilon}|\mathbf{x}) \log p(y|\mathbf{x}, \boldsymbol{\varepsilon})dyd\boldsymbol{\varepsilon}d\mathbf{x} + H(\mathcal{T}), \quad (9)$$

we can obtain the formal definition of the conditional task entropy given noise as $H(\mathcal{T}|\mathcal{E}) = - \int p(\mathbf{x})p(y, \boldsymbol{\varepsilon}|\mathbf{x}) \log p(y|\mathbf{x}, \boldsymbol{\varepsilon})dyd\boldsymbol{\varepsilon}d\mathbf{x}$.

3.2 Variational Approximation

To overcome *C1* proposed at the end of Section 1, we turn to maximize a variational lower bound of the mutual information by expanding $I(\mathcal{T}, \mathcal{E})$ as

$$I(\mathcal{T}, \mathcal{E}) \geq \int p(\mathbf{x})p(y, \boldsymbol{\varepsilon}|\mathbf{x}) \log q(y|\mathbf{x}, \boldsymbol{\varepsilon})dyd\boldsymbol{\varepsilon}d\mathbf{x} + \int -p(\mathbf{x})p(y|\mathbf{x}) \log p(y|\mathbf{x})dyd\mathbf{x} \quad (10)$$

$$= \int p(\mathbf{x})p(y, \boldsymbol{\varepsilon}|\mathbf{x}) \log q(y|\mathbf{x}, \boldsymbol{\varepsilon})dyd\boldsymbol{\varepsilon}d\mathbf{x} + H(\mathcal{T}), \quad (11)$$

where $q(y|\mathbf{x}, \boldsymbol{\varepsilon})$ is the tractable variational approximation of $p(y|\mathbf{x}, \boldsymbol{\varepsilon})$. Inequality (10) is derived from the non-negative property of Kullback-Leibler divergence (KL-divergence) [21],

$$KL(p||q) \geq 0 \Leftrightarrow \int p(x) \log p(x)dx \geq \int p(x) \log q(x)dx. \quad (12)$$

Since $\boldsymbol{\varepsilon}$ is the learnable variable and $H(\mathcal{T})$ is a constant term during optimization, the original problem is equivalent to maximize

$$\mathcal{L} = \int p(\mathbf{x})p(y, \boldsymbol{\varepsilon}|\mathbf{x}) \log q(y|\mathbf{x}, \boldsymbol{\varepsilon})dyd\boldsymbol{\varepsilon}d\mathbf{x} \quad (13)$$

$$= \int p(y, \mathbf{x})p(\boldsymbol{\varepsilon}|\mathbf{x}) \log q(y|\mathbf{x}, \boldsymbol{\varepsilon})dyd\boldsymbol{\varepsilon}d\mathbf{x} = \mathbb{E}_{\mathbf{x}, y \sim p(\mathbf{x}, y)} \int p(\boldsymbol{\varepsilon}|\mathbf{x}) \log q(y|\mathbf{x}, \boldsymbol{\varepsilon})d\boldsymbol{\varepsilon}. \quad (14)$$

Before the further discussion of \mathcal{L} , it should be emphasized that the conditional independence assumption $y \rightarrow \mathbf{x} \rightarrow \boldsymbol{\varepsilon}$, which is usually applied in related machine learning literatures, does not hold in this paper. From the mathematical perspective, if $y \rightarrow \mathbf{x} \rightarrow \boldsymbol{\varepsilon}$ is a Markov chain, then $p(y|\mathbf{x}, \boldsymbol{\varepsilon}) = p(y|\mathbf{x})$, which is contradictory with the π -noise.

We can form the Monte Carlo estimation of the expectation to avoid the direct computation of the integral in \mathcal{L} , which is formulated as

$$\mathcal{L} \approx \frac{1}{n} \sum_{i=1}^n \int p(\boldsymbol{\varepsilon}|y_i, \mathbf{x}_i) \log q(y_i|\mathbf{x}_i, \boldsymbol{\varepsilon})d\boldsymbol{\varepsilon} = \frac{1}{n} \sum_{i=1}^n \mathbb{E}_{\boldsymbol{\varepsilon} \sim p(\boldsymbol{\varepsilon}|y_i, \mathbf{x}_i)} \log q(y_i|\mathbf{x}_i, \boldsymbol{\varepsilon}). \quad (15)$$

Surprisingly, the challenge *C2* is also partially solved by avoiding sampling diverse y for \mathbf{x} . Although the above sampling may be biased, it is shown that this approximate method has achieved remarkable results from experiments.

The expectation can be also estimated by the Monte Carlo method to efficiently compute the integral of the continuous variable $\boldsymbol{\varepsilon}$. To ensure the backpropagation of gradient, we apply the well-known reparameterization trick [18] and reformulate $p(\boldsymbol{\varepsilon}|y_i, \mathbf{x}_i)d\boldsymbol{\varepsilon} = p(\boldsymbol{\varepsilon})d\boldsymbol{\varepsilon}$ where $\boldsymbol{\varepsilon} = \hat{g}_{\boldsymbol{\theta}}(\mathbf{x}_i, y_i, \boldsymbol{\varepsilon})$ is a learnable function of a supervised sample (\mathbf{x}_i, y_i) and a standard multivariate Gaussian random variable $\boldsymbol{\varepsilon} \sim p(\boldsymbol{\varepsilon}) = \mathcal{N}(0, \mathbf{I})$. Accordingly, the objective of variational π -noise (VPN) is

$$\max_{\boldsymbol{\phi}} \frac{1}{n} \sum_{i=1}^n \int p(\boldsymbol{\varepsilon}) \log q(y_i|\mathbf{x}_i, \hat{g}_{\boldsymbol{\theta}}(\mathbf{x}_i, y_i, \boldsymbol{\varepsilon}))d\boldsymbol{\varepsilon} = \frac{1}{n} \sum_{i=1}^n \mathbb{E}_{\boldsymbol{\varepsilon} \sim p(\boldsymbol{\varepsilon})} \log q(y_i|\mathbf{x}_i, \hat{g}_{\boldsymbol{\theta}}(\mathbf{x}_i, y_i, \boldsymbol{\varepsilon})). \quad (16)$$

The above objective can be further written as the Monte Carlo approximation form and the loss of VPN is formulated as

$$\min_{\phi} \mathcal{L}_{\text{VPN}} = -\frac{1}{n \cdot m} \sum_{i=1}^n \sum_{j=1}^m \log q(y_i | \mathbf{x}_i, \hat{g}_{\theta}(\mathbf{x}_i, y_i, \epsilon_{i,j})) \text{ where } \epsilon_{i,j} \sim p(\epsilon). \quad (17)$$

Finally, we formally present the relation between \mathcal{D}_{θ} and the function \hat{g}_{θ} , to provide the formulation of \mathcal{D}_{θ} defined at the beginning of Section 3, as follows

$$\mathcal{D}_{\theta}(\mathbf{x}_i, y_i) = p(\epsilon | \mathbf{x}_i, y_i) = \int_E^{(L)} p(\epsilon) d\epsilon, \text{ where } E = \{\epsilon | \hat{g}_{\theta}(\mathbf{x}_i, y_i, \epsilon) = \epsilon\}. \quad (18)$$

3.3 Positive-incentive Gaussian π -Noise

To be specific, we elaborate on how to set $p(\epsilon | y_i, \mathbf{x}_i)$ and $q(y_i | \mathbf{x}_i, \hat{g}_{\theta}(\mathbf{x}_i, y_i, \epsilon_{i,j}))$ used in practice. Note that $q(y_i | \mathbf{x}_i, \epsilon)$, the approximation of $p(y_i | \mathbf{x}_i, \epsilon)$, should be tractable. A simple but effective scheme is to model it by the probability output by the base model,

$$q(y_i | \mathbf{x}_i, \epsilon) = h_{\phi}(\mathbf{x}_i, \epsilon) = \text{softmax}(\hat{h}_{\phi}(\mathbf{x}_i, \epsilon)), \quad (19)$$

where $\hat{h}_{\phi}(\cdot)$ represents the neural network without the final decision layer. Clearly, most deep models for classification (*e.g.*, ResNet [22], ViT [23]) can be valid h_{ϕ} . With some simple additional modules, some contrastive models (*e.g.*, CLIP [24]) are also compatible with the proposed VPN generator. Although there are plenty of techniques (*e.g.*, Siamese network and concatenation) to simultaneously process both \mathbf{x} and ϵ and feed them to the base model, a simpler scheme, $\mathbf{x} + \epsilon$, is used in this paper. It is the most advantage to avoid refining the architecture of base models so that the VPN generator can be easily applied to any network.

$p(\epsilon | y_i, \mathbf{x}_i)$ is another crucial distribution. We assume that $p(\epsilon | y_i, \mathbf{x}_i)$ is an uncorrelated multivariate Gaussian distribution, *i.e.*,

$$p(\epsilon | y_i, \mathbf{x}_i) = \mathcal{N}(0, \Sigma_i), \text{ s.t. } \Sigma_i \in \mathbb{D}^d, \quad (20)$$

where \mathbb{D}^d represents the set of $d \times d$ diagonal matrices. The major benefit brought by the assumption of uncorrelation is the great reduction of the amount of parameters and burden of computation, *i.e.*, from $\mathcal{O}(d^2)$ to $\mathcal{O}(d)$. One may argue that ϵ acts more like a data augmentation due to that Σ is learned from \mathbf{x}_i . We, therefore, constrain the mean vector as 0, which is another crucial assumption in our paper. It effectively prevents the generator from falling into a trivial solution, $\mu = \mathbf{x}_i$ and $\Sigma = 0$. The constraint ensures that ϵ is a random disturbance. To limit the influence of noise, we can apply further limitations to it. For example, if π -noise obeys the multivariate Gaussian distribution, the simple restriction $\|\Sigma\| \leq C$ can efficiently constrain the intensity of ϵ .

Σ is the output of a neural network denoted by f_{θ} , *i.e.*, $\Sigma = f_{\theta}(\mathbf{x}, y)$. In summary, the generator module is composed of sampling and distribution parameter inference, *i.e.*, $G_{\theta} = \text{Sample} \circ f_{\theta}$. It should be emphasized that f_{θ} is a special module different from the existing networks, since it takes both \mathbf{x} and y as the input while the conventional neural networks only require \mathbf{x} as the input. We try to keep the original architectures of existing well-known networks for the sake of stable performance. For simplicity, we first convert (\mathbf{x}, y) to $\hat{\mathbf{x}} = \mathbf{x} + \gamma \cdot y$ and then feed it to networks. y serves as a bias and γ is a constant coefficient.

Following [18], we can sample m noises for each data point from a standard Gaussian distribution. The training algorithm is summarized in Algorithm 1. When testing an unseen sample, since the generator requires a label as input, we suppose that the sample belongs to some class Y and we can obtain a π -noise drawn from $p(\epsilon | \mathbf{x}, y = Y)$. Then the noise is fed to the base model with \mathbf{x} and $q(y = Y | \mathbf{x}, \epsilon)$ is computed. This process is repeated for every class in $|\mathcal{Y}|$ and the label with the largest probability will be the predicted class. The procedure is shown in Algorithm 2.

4 Experiments

In this section, we present experimental results to testify: (1) whether the base model benefits from training an additional VPN generator; (2) what kind of noise would be the π -noise that simplifies the task; (3) how to build a generator with proper architecture. As discussed in preceding sections, there are two modules involved in the experiments, base model and VPN generator, which are represented by h_{ϕ} and G_{θ} respectively.

Algorithm 1 Train base model and the VPN generator to generate Gaussian π -noise	Algorithm 2 Test a new sample with the trained VPN generator
<p>Input: Training set $\{(\mathbf{x}_i, y_i)\}_{i=1}^n$, batch size b, noise size m.</p> <p>Output: A generator $G_\theta = \text{Sample} \circ f_\theta$ and base model h_ϕ.</p> <p>Initialize the base model h_ϕ and VPN generator G_θ.</p> <p>for sampled mini-batch $\{(\mathbf{x}_k, y_k)\}_{k=1}^b$ do</p> <p style="padding-left: 20px;">for each (\mathbf{x}_k, y_k) do</p> <p style="padding-left: 40px;">$\Sigma_k = f_\theta(\mathbf{x}_k, y_k)$ where $\Sigma \in \mathbb{D}^d$.</p> <p style="padding-left: 40px;">Sample m noise $\{\epsilon_{k,j}\}_{j=1}^m$ for \mathbf{x}_k from $\mathcal{N}(0, \mathbf{I})$.</p> <p style="padding-left: 40px;">Reparameterization: $\forall j, \epsilon_{k,j} = \epsilon_{k,j} \odot \text{diag}(\Sigma_k)$.</p> <p style="padding-left: 20px;">end for</p> <p style="padding-left: 20px;">Obtain $\{(\mathbf{x}_k, y_k, \epsilon_{k,j})\}_{k,j}$. # Totally $m \times b$ triplets</p> <p style="padding-left: 20px;">Update θ and ϕ by minimizing \mathcal{L}_{VPN}.</p> <p>end for</p>	<p>Input: The trained h_ϕ and G_θ, a test sample \mathbf{x}.</p> <p>Output: Prediction y of \mathbf{x}.</p> <p>for each $Y \in \mathcal{Y}$ do</p> <p style="padding-left: 20px;"># Module $G_\theta = \text{Sample} \circ f_\theta$</p> <p style="padding-left: 20px;"># and $\epsilon_Y = G_\theta(\mathbf{x}, Y)$.</p> <p style="padding-left: 20px;">Compute $\Sigma_Y = f_\theta(\mathbf{x}, Y)$.</p> <p style="padding-left: 20px;">Sample $\epsilon_Y \sim \mathcal{N}(0, \Sigma_Y)$.</p> <p>end for</p> <p style="padding-left: 20px;"># Using $h_\phi(\mathbf{x}, \epsilon_Y)$ referring</p> <p style="padding-left: 20px;"># to Eq. (19)</p> <p style="padding-left: 20px;">$y \leftarrow \arg \max_Y q(y = Y \mathbf{x}, \epsilon_Y)$</p>

Table 1: Test accuracy: All base models h_ϕ are jointly trained with VPN generators G_θ .

$G_\theta \backslash h_\phi$	Fashion-MNIST				CIFAR-10			
	SR	DNN3	Res18	Res34	SR	DNN3	Res18	Res34
Baseline	74.97	81.57	90.23	90.86	39.08	46.92	79.51	80.88
Random	71.82	79.45	91.21	91.61	39.06	48.15	76.39	77.06
DNN3	76.34	81.79	91.69	91.97	39.36	48.76	80.27	83.60
DNN3 (No Noise)	76.34	81.83	91.74	92.06	39.47	49.07	80.87	83.78
ResNet18	67.63	82.19	74.02	86.92	39.34	50.15	79.93	74.29
ResNet18 (No Noise)	76.48	82.19	76.93	87.03	39.39	50.11	79.91	70.95

4.1 Implementation Details

Datasets Although the proposed VPN framework does not rely on any specific type of data and network, we conduct the experiments on vision datasets for the better visualization. The idea are verified on Fashion-MNIST [25], CIFAR-10 [26], and Tiny ImageNet (a subset of ImageNet [9]). Fashion-MNIST and CIFAR-10 contain 70,000 images belonging to 10 classes. The split of training-validation-test set is 50,000-10,000-10,000 Tiny ImageNet consists of 110,000 images belonging to 200 categories. There are 500 images for training, 50 images for validation, and 50 images for test in each category. The image size of Fashion-MNIST, CIFAR-10, and Tiny ImageNet are 28x28, 32x32, and 64x64, respectively. Remark that all input features are firstly scaled to $[0, 1]$ before they are fed to neural networks.

Settings of base model h_ϕ On Fashion-MNIST and CIFAR-10, the base models include a linear model, a shallow model, and two deep models. Totally 4 different models are employed as the base model in the experiments, including the softmax regression (SR) [27], 3-layer DNN (DNN3), ResNet18 [22], and ResNet34[22]. SR is a linear multi-class classifier extended from the logistic regression and is used to show that the VPN generator can be applied to any models provided that they can output $p(y|\mathbf{x})$. DNN3 serves as a shallow and simple multi-layer perceptron (MLP) composed of the form d -1024-1024- $|\mathcal{Y}|$. On Tiny MNIST, SR and DNN3 are omitted due to the lacking of representative capacity and a deeper network, ResNet50, is added.

Settings of VPN generator G_θ The VPN generator intends to generate Gaussian π -noise which is formally presented in Section 3.3. The Gaussian generator G_θ consists of two parts, sampling and parameter learning (denoted by f_θ). f_θ is also testified with both shallow and deep network, DNN3 and ResNet18. Similarly, DNN3 denotes a 3-layer MLP of the form d -1024-1024- d . Remark that the neuron number of the last layer is reduced from $d^2 + d$ to d owing to the assumption of the zero mean ($\boldsymbol{\mu} = 0$) and the uncorrelated variance ($\boldsymbol{\Sigma} \in \mathbb{D}^d$).

Ablation Settings To testify whether the VPN generator works, we train the base model without any augmentation on three datasets under the same settings, which is denoted by *Baseline*. We also

Table 2: Test accuracy: All generators are trained on fixed base models.

G_θ	h_ϕ	Fashion-MNIST				CIFAR-10			
		SR	DNN3	Res18	Res34	SR	DNN3	Res18	Res34
Baseline		74.97	81.57	90.23	90.86	39.08	46.92	79.51	80.88
DNN3		75.08	81.86	90.44	90.92	39.14	47.30	80.19	82.11
ResNet18		75.06	81.74	90.42	90.81	39.15	47.35	80.49	82.56

train the base models with the standard Gaussian noise, to validate whether the random Gaussian noise would lead to the same performance improvement. Specifically speaking, we randomly select 10% pixels and add standard Gaussian noise to them for every image. The corresponding results are denoted by *Random*. To alleviate the impact of randomness, the corresponding results are the averaged result over 5 individual experiments. We also test the prediction accuracy of base models, which are trained with generators, without feeding noise. The results are denoted by *No Noise*.

Hyperparameters Since how to tune the base model is not the core purpose of this paper, we simply set the number of epochs as 40 on all datasets. The learning rate is 0.001. To feed both x and y to the generator, we process them by $\hat{x} = x + \gamma \cdot y$ where y is encoded as the class index starting from 0 and $\gamma = 0.01 \times 1/|\mathcal{Y}|$. On Fashion-MNIST and CIFAR-10, a batch size of 256 is used. On Tiny ImageNet, the batch size is set as 128 to prevent the OOM exception. Another hyperparameter is the noise size m , the number of sampling noise during training. For the sake of training efficiency, we use $m = 1$ on all datasets. Therefore, we can run all codes on an NVIDIA GeForce RTX 3090Ti GPU. The source code is implemented under PyTorch 1.10.0 and provided in supplementary materials.

4.2 Performance Analysis

Overall, the experiments in this paper can be divided into two classes: (1) training generators with base models; (2) training generators after base models.

For the former case, the experimental results on Fashion-MNIST and CIFAR-10 are reported in Table 1 and the results on Tiny ImageNet are reported in Table 3. Firstly, the generator can promote the base model in most cases. Due to the training of generator, the accuracy increases by over 4% on Tiny ImageNet with $h_\phi = \text{ResNet-34}$ and $G_\theta = \text{ResNet-18}$.

Secondly, compared with the experiments with random Gaussian noise, we confirm that the augmentation by random Gaussian noise is unstable and the VPN generator is much more stable. It verifies the effectiveness of the idea of learning Gaussian noise. Thirdly, DNN3 is more stable than ResNet-18. It may be caused by the fact that deeper networks easily suffer from over-fitting. We also suspect that the information of π -noise may be easier to extract, compared with the visual semantic information, so that ResNet-18 may therefore suffer from over-fitting. Fourthly, after training base models and generators, it seems not necessary to generate π -noise for unseen samples in the test phase. It indirectly validates that the component generated by generators are not too intense and does not significantly change the original images. It is adequate to name it “noise”.

For the latter case, we show the results of training all generators on the trained base models in Table 2. Note that when testing a new sample, we sample a noise with the help of the trained G_θ so that it behaves differently from the trained base model. Surprisingly, *the accuracy improvement is even more stable compared with Table 1*. It may be owing to the high sensitivity of training neural networks, especially deep models. For example, ResNet-50 suffers from a clear degradation on Tiny ImageNet. It also implies that the generator may still have the potential to be further developed.

Convergence We show the convergence curves of loss, training accuracy, and test accuracy in Figure 2. From the figure, we find that the training on Tiny ImageNet is more stable compared

Table 3: Test accuracy on Tiny ImageNet: Base models and generators are simultaneously trained.

G_θ	h_ϕ	Res18	Res34	Res50
		Baseline	28.20	29.73
Random		32.18	32.30	35.21
DNN3		33.81	33.65	35.92
DNN3 (No Noise)		34.13	33.88	36.62
Res18		33.05	34.20	34.64
Res18 (No Noise)		32.42	34.20	34.64

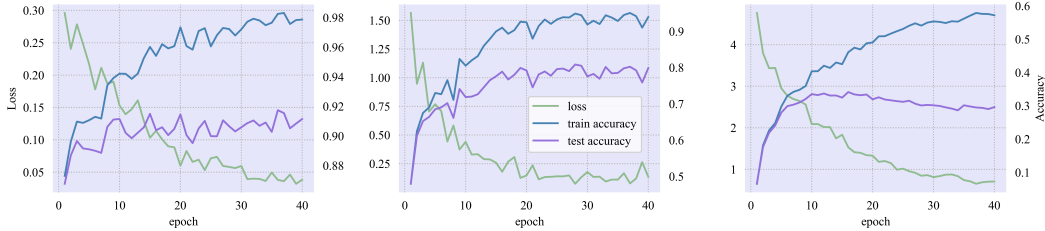


Figure 2: Convergence curve on Fashion-MNIST, CIFAR-10, and Tiny ImageNet, respectively. The base model is ResNet18 and the generator is DNN3.

with Fashion-MNIST and CIFAR-10. The oscillation of the curves may be caused by the setting of $m = 1$. As shown in next paragraph, this setting ensures the fast training of generator without apparent performance loss.

Impact of noise size m The impact of the number of generated noises, m in Algorithm 1, is also investigated and the results are shown in Figure 3. The generator with different m for training achieves similar final accuracies. Larger m leads to faster convergence. When the computing resources is limited, we suggest to simply set $m = 1$. It should be pointed out we use $m = 1$ in all other experiments.

4.3 Visualization

To answer the question about “what kind of noise would be the π -noise that simplifies the task”, we visualize the variance of the learned multivariate Gaussian noise as a heatmap and a noise drawn from the distribution in Figure 4. We show two images of FashionMNIST and CIFAR-10 while 5 images from Tiny ImageNet are exhibited. From Figure 4, it is easy to find that the learned π -noise differs on these three datasets.

Since Fashion-MNIST is a dataset of grayscale images without noisy background, it is easy to theoretically speculate that changing background would be helpless for decreasing the task entropy defined in Eq. (2), *i.e.*, $H(\mathcal{T}) = H(\mathcal{T}|\mathcal{E})$. Therefore, the π -noise can only enhance the pixels related to objects. The first and second columns in Figure 4 strongly supports our guess and verifies that the proposed VPN indeed tries to minimize the conditional task entropy $H(\mathcal{T}|\mathcal{E})$.

On CIFAR-10 and ImageNet consisting of colorful images, the ideal π -noise should blur the background irrelevant to the main object so that $p(y|x)$ can approach the one-hot distribution and the conditional task entropy can decrease. From Figure 4, we find that the generator aims to disturb the pixels related to background. Surprisingly, on more complicated images from Tiny ImageNet, the generator precisely distinguishes which pixels are irrelevant. For instance, it adds intense noise to the flower in the butterfly image. The flower is the ingredient that is most similar to the butterfly. From the heatmap images of flagstaff and sea lion, the heatmap highly matches the background and the outline of objects is almost detected. Even though the base model is not well-trained on Tiny ImageNet, the generator has already distinguished the ingredients in images. Therefore, the π -noise may provide a new scheme for segmentation and an idea to bridge the classical image recognition and image segmentation.

It should be pointed out that only part of background is detected. For example, the seventh image is labeled by flagstaff instead of flag, but only the sky is recognized as the irrelevant ingredient. It may be caused by the lacking of training data (only 500 images are used for training).

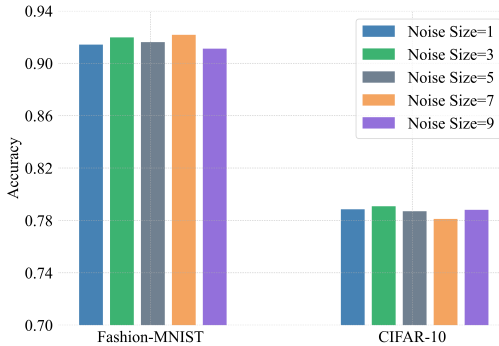


Figure 3: Impact of noise size m on Fashion-MNIST and CIFAR-10. The base model and generator are ResNet18 and DNN3, respectively.

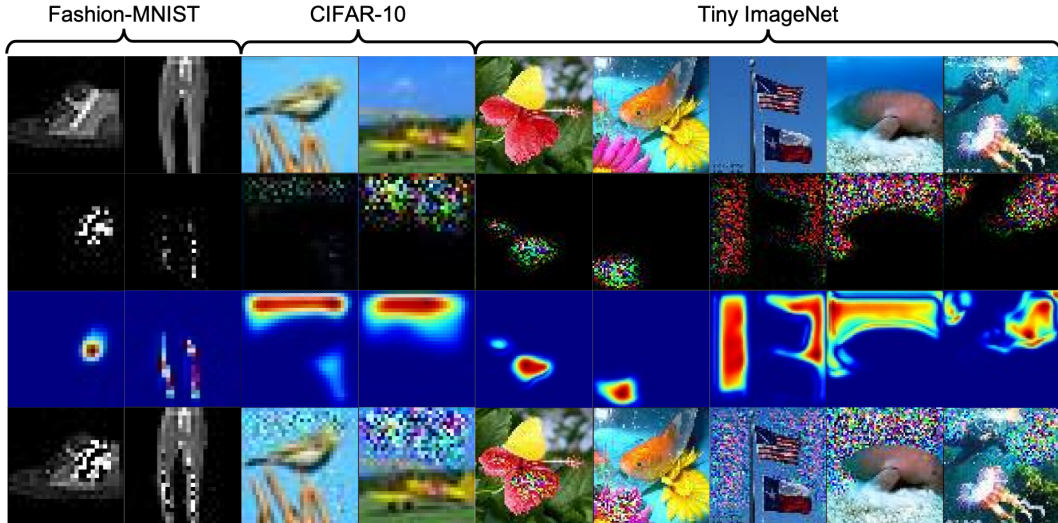


Figure 4: Visualization of generated π -noise on some images. The first line is the original image, the second line shows the generated noise, the third line is the heatmap of variance related to each pixel, and the bottom line is the image added with π -noise. In the fifth image labeled by butterfly, the flower which is most similar to butterfly is disturbed by intense noise so that the recognition task is significantly simplified.

In sum, the visualization verifies that the VPN generator indeed helps to promote the base model and it meets our expectation of the task entropy defined in Eq. (2).

5 Future Works

Owing to the Monte Carlo estimation, the π -noise generator can be trained by sampling without knowing exact $p(y|\mathbf{x})$. However, since each data point only has one label in datasets for *single-label* classification, we will never get different y for a sample \mathbf{x} . This will lead to a biased estimation of expectations. One may argue that multi-label datasets should be used for training models. The purpose of defining $p(y|\mathbf{x})$ on single-label classification is to measure the task complexity. There should be a preference for different classes for \mathbf{x} . However, even on multi-label datasets, $p(y|\mathbf{x})$ is still not provided. It is still biased to simply set $p(y|\mathbf{x})$ as a uniform distribution since there should be one or two primary labels rather than treating all labels equally. The rationale is the lacking of suitable datasets that could provide preference ($p(y|\mathbf{x})$) of different classes but is still designed for classic single-label classification. Therefore, it is the principal work to collect a dataset to train π -noise generators unbiasedly.

In Section 3.3, we discuss how to model $q(y|\mathbf{x}, \varepsilon)$ and $p(\varepsilon|\mathbf{x}, y)$, which both require two inputs. In this paper, they are processed by the simple summation operation to prevent the potential over-fitting risk. However, too simple operations may limit the performance and result in bias. More sophisticated techniques, especially for $p(\varepsilon|\mathbf{x}, y)$, deserve to be studied. An ideal scheme is developing a module $\varphi : \mathcal{X} \times \mathcal{Y} \mapsto \mathcal{X}'$ where $\dim \mathcal{X}' = \dim \mathcal{X}$. It is crucial to properly use y without over-fitting as the input of a network to generate deep representation.

6 Conclusion

In this paper, we propose the Variational Positive-incentive Noise (VPN), an approximate method to learn π -noise via variational inference, following the framework of π -noise [1]. We validate the efficacy of the idea about generating random noise to enhance the classifier. The π -noise generator always promotes the base model no matter whether to train the base model with the generator or not. It implies that the VPN generator is a flexible module independent of the existing classifiers. From the visualization of generated noise, the generator aims to blur the background of complicated images, which highly meets our expectations of the defined task entropy.

References

- [1] Xuelong Li. Positive-incentive noise. *IEEE Transactions on Neural Networks and Learning Systems*, pages 1–7, 2022.
- [2] Pascal Vincent, Hugo Larochelle, Isabelle Lajoie, Yoshua Bengio, and Pierre-Antoine Manzagol. Stacked denoising autoencoders: Learning useful representations in a deep network with a local denoising criterion. *Journal of Machine Learning Research*, 11:3371–3408, 2010.
- [3] Nitish Srivastava, Geoffrey E. Hinton, Alex Krizhevsky, Ilya Sutskever, and Ruslan Salakhutdinov. Dropout: a simple way to prevent neural networks from overfitting. *Journal of Machine Learning Research*, 15(1):1929–1958, 2014.
- [4] Christian Szegedy, Wojciech Zaremba, Ilya Sutskever, Joan Bruna, Dumitru Erhan, Ian J. Goodfellow, and Rob Fergus. Intriguing properties of neural networks. In *2nd International Conference on Learning Representations, ICLR 2014, Banff, AB, Canada, April 14-16, 2014, Conference Track Proceedings*, 2014.
- [5] Ian J. Goodfellow, Jean Pouget-Abadie, Mehdi Mirza, Bing Xu, David Warde-Farley, Sherjil Ozair, Aaron C. Courville, and Yoshua Bengio. Generative adversarial nets. In *Advances in Neural Information Processing Systems 27: Annual Conference on Neural Information Processing Systems 2014, December 8-13 2014, Montreal, Quebec, Canada*, pages 2672–2680, 2014.
- [6] Michael Gutmann and Aapo Hyvärinen. Noise-contrastive estimation: A new estimation principle for unnormalized statistical models. In *Proceedings of the Thirteenth International Conference on Artificial Intelligence and Statistics, AISTATS 2010, Chia Laguna Resort, Sardinia, Italy, May 13-15, 2010*, volume 9, pages 297–304, 2010.
- [7] Jonathan Ho, Ajay Jain, and Pieter Abbeel. Denoising diffusion probabilistic models. In Hugo Larochelle, Marc’Aurelio Ranzato, Raia Hadsell, Maria-Florina Balcan, and Hsuan-Tien Lin, editors, *Advances in Neural Information Processing Systems 33: Annual Conference on Neural Information Processing Systems 2020, NeurIPS 2020, December 6-12, 2020, virtual*, 2020.
- [8] Rafael Müller, Simon Kornblith, and Geoffrey E. Hinton. When does label smoothing help? In *Advances in Neural Information Processing Systems 32: Annual Conference on Neural Information Processing Systems 2019, NeurIPS 2019, December 8-14, 2019, Vancouver, BC, Canada*, pages 4696–4705, 2019.
- [9] Olga Russakovsky, Jia Deng, Hao Su, Jonathan Krause, Sanjeev Satheesh, Sean Ma, Zhiheng Huang, Andrej Karpathy, Aditya Khosla, Michael Bernstein, Alexander C. Berg, and Li Fei-Fei. ImageNet Large Scale Visual Recognition Challenge. *International Journal of Computer Vision (IJCV)*, 115(3):211–252, 2015.
- [10] Grigorios Tsoumakas and Ioannis Katakis. Multi-label classification: An overview. *Int. J. Data Warehous. Min.*, 3(3):1–13, 2007.
- [11] Ekin D. Cubuk, Barret Zoph, Dandelion Mané, Vijay Vasudevan, and Quoc V. Le. Autoaugment: Learning augmentation strategies from data. In *IEEE Conference on Computer Vision and Pattern Recognition, CVPR 2019, Long Beach, CA, USA, June 16-20, 2019*, pages 113–123. Computer Vision Foundation / IEEE, 2019.
- [12] Aäron van den Oord, Yazhe Li, and Oriol Vinyals. Representation learning with contrastive predictive coding. *CoRR*, abs/1807.03748, 2018.
- [13] Ting Chen, Simon Kornblith, Mohammad Norouzi, and Geoffrey E. Hinton. A simple framework for contrastive learning of visual representations. In *Proceedings of the 37th International Conference on Machine Learning, ICML 2020, 13-18 July 2020, Virtual Event*, volume 119 of *Proceedings of Machine Learning Research*, pages 1597–1607. PMLR, 2020.
- [14] Takeru Miyato, Shin-ichi Maeda, Masanori Koyama, Ken Nakae, and Shin Ishii. Distributional smoothing with virtual adversarial training. *arXiv preprint arXiv:1507.00677*, 2015.
- [15] Weihua Hu, Takeru Miyato, Seiya Tokui, Eiichi Matsumoto, and Masashi Sugiyama. Learning discrete representations via information maximizing self-augmented training. In *Proceedings of the 34th International Conference on Machine Learning, ICML 2017, Sydney, NSW, Australia, 6-11 August 2017*, volume 70, pages 1558–1567, 2017.
- [16] Ian J. Goodfellow, Jonathon Shlens, and Christian Szegedy. Explaining and harnessing adversarial examples. In *3rd International Conference on Learning Representations, ICLR 2015, San Diego, CA, USA, May 7-9, 2015, Conference Track Proceedings*, 2015.

- [17] Jiawei Su, Danilo Vasconcellos Vargas, and Kouichi Sakurai. One pixel attack for fooling deep neural networks. *IEEE Trans. Evol. Comput.*, 23(5):828–841, 2019.
- [18] Diederik P Kingma and Max Welling. Auto-encoding variational bayes. In *ICLR*, 2014.
- [19] Alexander A. Alemi, Ian Fischer, Joshua V. Dillon, and Kevin Murphy. Deep variational information bottleneck. In *5th International Conference on Learning Representations, ICLR 2017, Toulon, France, April 24-26, 2017, Conference Track Proceedings*, 2017.
- [20] Tailin Wu, Hongyu Ren, Pan Li, and Jure Leskovec. Graph information bottleneck. In *Advances in Neural Information Processing Systems 33: Annual Conference on Neural Information Processing Systems 2020, NeurIPS 2020, December 6-12, 2020, virtual*, 2020.
- [21] Imre Csiszár. I-divergence geometry of probability distributions and minimization problems. *The annals of probability*, pages 146–158, 1975.
- [22] Kaiming He, Xiangyu Zhang, Shaoqing Ren, and Jian Sun. Deep residual learning for image recognition. In *2016 IEEE Conference on Computer Vision and Pattern Recognition, CVPR 2016, Las Vegas, NV, USA, June 27-30, 2016*, pages 770–778. IEEE Computer Society, 2016.
- [23] Alexey Dosovitskiy, Lucas Beyer, Alexander Kolesnikov, Dirk Weissenborn, Xiaohua Zhai, Thomas Unterthiner, Mostafa Dehghani, Matthias Minderer, Georg Heigold, Sylvain Gelly, Jakob Uszkoreit, and Neil Houlsby. An image is worth 16x16 words: Transformers for image recognition at scale. In *9th International Conference on Learning Representations, ICLR 2021, Virtual Event, Austria, May 3-7, 2021*, 2021.
- [24] Alec Radford, Jong Wook Kim, Chris Hallacy, Aditya Ramesh, Gabriel Goh, Sandhini Agarwal, Girish Sastry, Amanda Askell, Pamela Mishkin, Jack Clark, Gretchen Krueger, and Ilya Sutskever. Learning transferable visual models from natural language supervision. In *Proceedings of the 38th International Conference on Machine Learning, ICML 2021, 18-24 July 2021, Virtual Event*, volume 139, pages 8748–8763. PMLR, 2021.
- [25] Han Xiao, Kashif Rasul, and Roland Vollgraf. Fashion-mnist: a novel image dataset for benchmarking machine learning algorithms. *arXiv preprint arXiv:1708.07747*, 2017.
- [26] Alex Krizhevsky, Geoffrey Hinton, et al. Learning multiple layers of features from tiny images. 2009.
- [27] Christopher M Bishop and Nasser M Nasrabadi. *Pattern recognition and machine learning*, volume 4. Springer, 2006.